Generalized Injection Shift Factors

Yu Christine Chen, *Member, IEEE*, Sairaj V. Dhople, *Member, IEEE*,
Alejandro D. Domínguez-García, *Member, IEEE*, and Peter W. Sauer, *Life Fellow, IEEE*

***Abstract*—Generalized injection shift factors (ISFs) are the sensitivities of active-power line flows to active-power bus injections. They are computed without designating an artifactual slack bus in the power network; therefore, conceptually, they reflect sensitivities of power flows more accurately than conventional ISFs, the values of which depend on the choice of the slack bus. This paper derives analytical closed-form expressions for generalized ISFs from a perturbative analysis of the AC circuit equations. In addition, they are computed from a system of linear equations that arise from high-frequency synchronized measurements collected from phasor measurement units. As an application, generalized ISFs are used to predict active-power line flows during the transient period following a contingency by leveraging inertial and governor power flows over appropriate time horizons.**

***Index Terms*—Distribution factor, injection shift factor, monitoring, phasor measurement units, sensitivity.**

I. Introduction

POWER system operational reliability is monitored and maintained with a suite of online static and dynamic security-assessment tools that allow operators to assess whether or not the system is capable of withstanding a wide variety of disturbances, such as sudden loss of a generator or load. Dynamic security assessment tools indicate the ability of the system to withstand transients induced by disturbances prior to reaching steady-state operation at a new operating point [1]. On the other hand, static security assessment tools examine the system in steady-state operation.

A common security assessment tool is real-time $N-1$ contingency analysis, in which operators determine whether or not the system would meet operational reliability requirements in case of an outage in any one particular asset [2]. With an accurate model of the system, operators can perform the $N-1$ security analysis by repeatedly solving the nonlinear power flow equations. However, for a large power system with many possible contingencies, this process is computationally expensive, and therefore could take prohibitively long periods of time. An alternative is to use an estimate of the current operating point together with linear sensitivity distribution factors (DFs) in order to predict values of different variables following the occurrence of a contingency [3]. For example, the so-called power transfer distribution factor (PTDF) approximates the changes in active-power line flows due to an exchange of active power between two buses. In general, such line flow DFs can all be derived from the injection shift factor (ISF), which approximates the change in active-power flow across a transmission line due to a change in active-power generation or load at a particular bus.

In this paper, we develop the notion of a *generalized* ISF. Computed via a perturbative analysis of the AC circuit equations around a particular operating point, the generalized ISF is agnostic to the location (and even existence) of a slack bus. Indeed, the concept of the generalized ISF represents an important step in removing the dependence on slack bus location in steady-state power system studies. Additionally, leveraging results from previous work in [4], we estimate generalized ISFs by using real-time measurements without relying on an offline model of the system. Such measurement-based methods have been shown to be robust to undetected system-topology and operating-point changes [4]. The proposed generalized ISFs are utilized—based on the propagation of disturbances over time-scales for which inertial and governor power flows are valid [5]—to predict active-power line flows during the transient period following a disturbance.

Conventional ISFs are computed by linearizing the power flow equations around an operating point with a designated slack-bus location; then, they can be used to predict post-contingency steady-state active-power line flows [6]. The generalized ISFs presented in this work offer three compelling advantages over conventional ISFs. First, conventional ISF values differ depending on the choice of slack bus [7]. This is because conventional ISFs are derived from the power flow equations formulated by designating a slack bus, with the corresponding generator assumed to compensate for any power imbalances in the system. Second, the computation of conventional ISFs relies on an accurate model of the system, which may not be available due to poor records or erroneous telemetry from remotely monitored circuit breakers [8]. On the other hand, generalized ISFs can be computed from high-frequency synchronized measurements collected from phasor measurement units (PMUs). Finally, traditionally, ISFs (and DFs in general) have been used exclusively to verify that operational reliability requirements are met (see, e.g., [6]–[10]). Based on the propagation of disturbances over time-scales for which inertial and governor power flows are valid, we estimate active-power line flow limit violations not only at the post-contingency steady-state operating point, but also

The work of S. V. Dhople was supported in part by the National Science Foundation under CAREER award ECCS-1453921, and in part by a Minnesota's Discovery, Research and Innovation Economy grant. The work of A. D. Domínguez-García and P. W. Sauer was supported in part by the U.S. Department of Energy under the Consortium for Electric Reliability Technology Solutions, and in part by the Power Systems Engineering Research Center.

Y. C. Chen is with the Department of Electrical and Computer Engineering at the University of British Columbia, Vancouver, BC, V6T 1Z4, Canada. E-mail: chen@ECE.UBC.CA.

S. V. Dhople is with the Department of Electrical and Computer Engineering at the University of Minnesota, Minneapolis, MN, 55455, USA. E-mail: sdhople@UMN.EDU.

A. D. Domínguez-García and P. W. Sauer are with the Department of Electrical and Computer Engineering at the University of Illinois at Urbana-Champaign, Urbana, IL, 61801, USA. E-mails: {aledan, psauer}@ILLINOIS.EDU.

during the post-disturbance transient period.

This paper builds on preliminary work reported in [11], and enhances it in several directions. First, from a circuit-theoretic vantage point, we establish an analytical derivation for generalized ISFs that does not depend on the location of the slack bus. The process uncovers and formalizes intuitive connections between power-flow and current-flow sensitivity factors. Furthermore, by revisiting assumptions underlying the definition of widely accepted power system linear sensitivity factors, we extend the utility of power-flow sensitivities to large-scale power-system dynamic operational reliability monitoring. Finally, to demonstrate these aspects, we show how generalized ISFs can predict post-contingency transient line flows via case studies involving the simplified Western Electricity Coordinating Council (WECC) and the New England test systems.

The remainder of the paper is organized as follows. In Section II, we establish mathematical notation, introduce voltage phase-angle and magnitude sensitivities, define the conventional ISFs, and describe the conventional model-based method to obtain them. In Section III, we define the generalized ISFs and provide model- and measurement-based methods to obtain them. Generalized ISFs, as we show in Section IV, can be manipulated to recover conventional ISFs, and to predict transient active-power line flows after a disturbance. In Section V, we illustrate applications of generalized ISFs via case studies involving the WECC 3-machine 9-bus and the New England 10-machine 39-bus test systems. Finally, concluding remarks are provided in Section VI.

II. Preliminaries

This section first introduces the notation and power system model used in the remainder of the paper. Next, we derive sensitivities of bus-voltage phase-angles and magnitudes with respect to active-power bus injections, which are used to compute conventional ISFs. Finally, we provide an example to motivate the need for generalized ISFs.

A. Notation and Power System Model

Matrix transpose will be denoted by $(\cdot)^{\mathrm{T}}$, complex conjugate by $(\cdot)^*$, complex-conjugate transposition by $(\cdot)^{\mathrm{H}}$, real and imaginary parts of a complex number by $\mathrm{Re}\{\cdot\}$ and $\mathrm{Im}\{\cdot\}$, respectively, and $\mathrm{j} := \sqrt{-1}$. A diagonal matrix formed with entries of the vector x is denoted by $\mathrm{diag}(x)$; and $\mathrm{diag}(x/y)$ forms a diagonal matrix with the ith entry given by x_i/y_i, where x_i and y_i are the ith entries of vectors x and y, respectively. The spaces of $N \times 1$ real-valued and complex-valued vectors are denoted by $\mathbb{R}^N$ and $\mathbb{C}^N$, respectively. Given a vector function $f(x) = [f_1(x), \ldots, f_M(x)]^{\mathrm{T}} : \mathbb{R}^N \to \mathbb{R}^M$, $\nabla_x f(x)$ returns the $M \times N$ Jacobian matrix $[\nabla_x f_1(x)^{\mathrm{T}}, \ldots, \nabla_x f_M(x)^{\mathrm{T}}]^{\mathrm{T}}$, where, for each $i = 1, \ldots, M$, the gradient $\nabla_x f_i(x) = [\partial f_i(x)/\partial x_1, \ldots, \partial f_i(x)/\partial x_N]$. The $N \times N$ identity matrix is denoted by I_N. The $M \times N$ matrices with all zeros and ones are denoted by $0_{M\times N}$ and $1_{M\times N}$, respectively; e_i denotes a column vector of all zeros except with the ith entry equal to 1; and e_{ij} denotes a column vector of all zeros except with the ith and jth entries equal to 1 and -1, respectively. For a vector $x = [x_1, \ldots, x_N]^{\mathrm{T}}$, $x_i \in [-\pi, \pi]$ $\forall$ $i = 1, \ldots, N$, $\cos(x) := [\cos(x_1), \ldots, \cos(x_N)]^{\mathrm{T}}$ and $\sin(x) := [\sin(x_1), \ldots, \sin(x_N)]^{\mathrm{T}}$. Finally, $\Pi_\ell := [e_1, \ldots, e_{\ell-1}, e_{\ell+1}, \ldots, e_N] \in \mathbb{R}^{N\times N-1}$.

Consider a power system with N buses, and let $\mathcal{L}$ denote the set of transmission lines and $\mathcal{N}$ the set of buses in the system. Denote the bus admittance matrix by $Y \in \mathbb{C}^{N\times N}$. Further, let $V = [V_1, \ldots, V_N]^{\mathrm{T}} = |V|\angle\theta$, where $V_i = |V_i|\angle\theta_i \in \mathbb{C}$ represents the voltage phasor at bus i, and let $I = [I_1, \ldots, I_N]^{\mathrm{T}}$, where $I_i \in \mathbb{C}$ denotes the current injected into bus i (through a path not included in Y). Then, Kirchhoff's current law for the buses in the power system can be compactly represented in matrix-vector form as follows:

$$I = YV. \tag{1}$$

In (1), $Y \in \mathbb{C}^{N\times N}$ is the admittance matrix defined as

$$[Y]_{mn} := \begin{cases} y_m + \sum_{(m,k)\in\mathcal{L}} y_{mk}, & \text{if } m = n, \\ -y_{mn}, & \text{if } (m,n) \in \mathcal{L}, \\ 0, & \text{otherwise}, \end{cases} \tag{2}$$

where $y_m = g_m + \mathrm{j}b_m = y_{mm} + \sum_{(m,k)\in\mathcal{N}_m} y^{\mathrm{sh}}_{mk}$ denotes the total shunt admittance connected to bus m with $\mathcal{N}_m$ representing the set of neighbours of bus m and $y_{mm} \in \mathbb{C}$ any passive shunt elements connected to bus m.

Denote the vector of complex-power bus injections by $S = [S_1, \ldots, S_N]^{\mathrm{T}} = P + \mathrm{j}Q$, with $P = [P_1, \ldots, P_N]^{\mathrm{T}}$ and $Q = [Q_1, \ldots, Q_N]^{\mathrm{T}}$. [By convention, P_i and Q_i are positive for generators and negative for loads.] Then, complex-power bus injections can be compactly written as

$$S = \mathrm{diag}\,(V)\, I^*. \tag{3}$$

The bus-voltage angles are collected in the vector $\theta = [\theta_1, \ldots, \theta_N]^{\mathrm{T}}$, $\theta_i \in [-\pi, \pi]$. The following auxiliary bus-voltage-angle and power related variables will be useful:

$$\begin{aligned} &\theta^m := \theta - \theta_m 1_{N\times 1}, \quad \widetilde{\theta}^m := \Pi_m^{\mathrm{T}} \theta^m, \\ &\widetilde{P}^m := \Pi_m^{\mathrm{T}} P, \quad \widetilde{Q}^m := \Pi_m^{\mathrm{T}} Q, \end{aligned} \tag{4}$$

where θ^m is obtained by setting the system angle reference as θ_m (the voltage angle at bus m). In (4), $\widetilde{\theta}^m$, $\widetilde{P}^m$, and $\widetilde{Q}^m$ denote the $(N-1)$-dimensional vectors that result from removing the mth entry of the N-dimensional vectors θ^m, P, and Q, respectively. For example, suppose $N = 3$, and $\theta = [\theta_1, \theta_2, \theta_3]^{\mathrm{T}}$. For $m = 2$, it follows that $\theta^2 = [\theta_1 - \theta_2, 0, \theta_3 - \theta_2]^{\mathrm{T}}$, and $\widetilde{\theta}^2 = [\theta_1 - \theta_2, \theta_3 - \theta_2]^{\mathrm{T}}$.

B. Bus-voltage Phase-angle and Magnitude Sensitivities

Let the angle reference be established by the voltage phase angle at bus m. Then, leveraging the definitions in (4), the power-flow equations can be written compactly as follows:

$$f^m\left(\widetilde{\theta}^m, |V|, \widetilde{P}^m, Q\right) = 0_{(2N-1)\times 1}, \tag{5}$$

where the superscript m indicates that f^m is formulated by setting the angle reference to bus m. In (5), the dependence on network parameters, such as line series and shunt impedances, is implicit in the formulation of the function f^m.

Denote the solution to (5) by $(\widetilde{\theta}^m_\star, |V_\star|, \widetilde{P}^m_\star, Q_\star)$, and assume f^m is continuously differentiable with respect to $\widetilde{\theta}^m$, $|V|$, $\widetilde{P}^m$, and Q at $(\widetilde{\theta}^m_\star, |V_\star|, \widetilde{P}^m_\star, Q_\star)$. Let $\widetilde{\theta}^m = \widetilde{\theta}^m_\star + \Delta\widetilde{\theta}^m$, $|V| = |V_\star| + \Delta|V|$, $\widetilde{P}^m = \widetilde{P}^m_\star + \Delta\widetilde{P}^m$, and $Q = Q_\star + \Delta Q$. Then, by assuming that $\Delta\widetilde{\theta}^m$, $\Delta|V|$, $\Delta\widetilde{P}^m$, and ΔQ are sufficiently small, we can approximate (5) as

$$f^m\left(\widetilde{\theta}^m, |V|, \widetilde{P}^m, Q\right) \approx f^m\left(\widetilde{\theta}^m_\star, |V_\star|, \widetilde{P}^m_\star, Q_\star\right) + J_m \begin{bmatrix}\Delta\widetilde{\theta}^m \\ \Delta|V|\end{bmatrix} + D_m\Delta\widetilde{P}^m + E_m\Delta Q, \tag{6}$$

where

$$\begin{aligned} J_m &= \nabla_{[\widetilde{\theta}^m, |V|]} f^m\left(\widetilde{\theta}^m, |V|, \widetilde{P}^m, Q\right)\Big|_{(\widetilde{\theta}^m_\star, |V_\star|, \widetilde{P}^m_\star, Q_\star)} \\ D_m &= \nabla_{\widetilde{P}^m} f^m\left(\widetilde{\theta}^m, |V|, \widetilde{P}^m, Q\right)\Big|_{(\widetilde{\theta}^m_\star, |V_\star|, \widetilde{P}^m_\star, Q_\star)} \\ E_m &= \nabla_{Q} f^m\left(\widetilde{\theta}^m, |V|, \widetilde{P}^m, Q\right)\Big|_{(\widetilde{\theta}^m_\star, |V_\star|, \widetilde{P}^m_\star, Q_\star)}. \end{aligned} \tag{7}$$

The subscript m for the quantities J_m, D_m, and E_m indicates that they are obtained by setting the angle reference to bus m.

Since $(\widetilde{\theta}^m_\star, |V_\star|, \widetilde{P}^m_\star, Q_\star)$ is a solution to (5), then $f^m(\widetilde{\theta}^m_\star, |V_\star|, \widetilde{P}^m_\star, Q_\star) = 0_{(2N-1)\times 1}$. Also, for all application studies in the paper, we assume power flow balance is satisfied, which requires that $f^m(\widetilde{\theta}^m, |V|, \widetilde{P}^m, Q) = 0_{(2N-1)\times 1}$. Furthermore, $\Delta\widetilde{\theta}^m$, $\Delta|V|$, $\Delta\widetilde{P}^m$, and ΔQ are assumed to be small. With these in mind, it follows from (6) that

$$0 \approx J_m \begin{bmatrix}\Delta\widetilde{\theta}^m \\ \Delta|V|\end{bmatrix} + D_m\Delta\widetilde{P}^m + E_m\Delta Q. \tag{8}$$

In addition, since J_m is the Jacobian of the power flow equations evaluated at a nominal non-stressed operating point, we assume it is invertible around $(\widetilde{\theta}^m_\star, |V_\star|, \widetilde{P}^m_\star, Q_\star)$, so we can rearrange terms in (8) to obtain

$$\begin{aligned} \begin{bmatrix}\Delta\widetilde{\theta}^m \\ \Delta|V|\end{bmatrix} &\approx -J_m^{-1}\left(D_m\Delta\widetilde{P}^m + E_m\Delta Q\right) \\ &= -J_m^{-1}\left(D_m\Pi_m^{\mathrm{T}}\Delta P + E_m\Delta Q\right), \end{aligned} \tag{9}$$

where the second equality in (9) follows from (4).

C. Conventional Injection Shift Factors

Denote, by $\Psi^\ell_{(m,n),i}$, the ISF of line $(m,n) \in \mathcal{L}$ (assume positive real power flow from bus m to n measured at bus m) with respect to bus i, which is the linear approximation of the sensitivity of the active power flow in line (m,n) with respect to the active-power injection at bus i, *with the slack bus location specified* as bus ℓ. In the conventional power flow formulation, the slack bus sets the angle reference, and the generator connected to it absorbs any power imbalance in the system. With this assumption in place, similar to (5), the power flow equations can be written compactly as

$$f^\ell\left(\widetilde{\theta}^\ell, |V|, \widetilde{P}^\ell, Q\right) = 0_{(2N-1)\times 1}. \tag{10}$$

Following an analogous development as in (5)–(9), where all instances of m are substituted with ℓ, and neglecting ΔQ by setting $\Delta Q = 0_{N\times 1}$, (9) becomes

$$\begin{bmatrix}\Delta\widetilde{\theta}^\ell \\ \Delta|V|\end{bmatrix} \approx -J_\ell^{-1} D_\ell \Delta\widetilde{P}^\ell. \tag{11}$$

Denote the active-power injection at bus i and flow in line (m,n) by P_i and $P_{(m,n)}$, respectively. Further, assume all quantities in the system remain constant except a small change in P_i, denoted by ΔP_i. Denote the resulting change in $P_{(m,n)}$ by $\Delta P_{(m,n),i}$. Then, define

$$\Psi^\ell_{(m,n),i} := \frac{\partial P_{(m,n)}}{\partial P_i} \approx \frac{\Delta P_{(m,n),i}}{\Delta P_i}. \tag{12}$$

Conventional ISFs can be computed with a power flow model of the system obtained offline. We begin by expressing the current through line $(m,n) \in \mathcal{L}$ as

$$I_{(m,n)} = y_{(m,n)}(V_m - V_n) + y^{\mathrm{sh}}_{(m,n)} V_m, \tag{13}$$

where $y_{(m,n)} \in \mathbb{C}\backslash\{0\}$ is the admittance of the line connecting buses m and n, and $y^{\mathrm{sh}}_{(m,n)} \in \mathbb{C} \setminus \{0\}$ is the shunt admittance at bus m. Denote, by $S_{(m,n)} = P_{(m,n)} + \mathrm{j}Q_{(m,n)}$, the complex power flowing across line (m,n), which is expressed as

$$S_{(m,n)} = V_m I^*_{(m,n)}. \tag{14}$$

Substituting (13) into (14), and isolating the real part, we obtain

$$P_{(m,n)} = \mathrm{Re}\{S_{(m,n)}\} =: h_{(m,n)}(\widetilde{\theta}^\ell, |V|). \tag{15}$$

Under the same small $\Delta\widetilde{\theta}^\ell$ and $\Delta|V|$ assumption used to derive (11), we obtain an expression for small variations $\Delta P_{(m,n)}$ due to $\Delta\widetilde{\theta}^\ell$ and $\Delta|V|$, as follows:

$$\Delta P_{(m,n)} \approx [w_1, w_2] \begin{bmatrix}\Delta\widetilde{\theta}^\ell \\ \Delta|V|\end{bmatrix}, \tag{16}$$

where

$$\begin{aligned} w_1 &= \nabla_{\widetilde{\theta}^\ell} h_{(m,n)}\left(\widetilde{\theta}^\ell, |V|\right)\Big|_{(\widetilde{\theta}^\ell_\star, |V_\star|)}, \\ w_2 &= \nabla_{|V|} h_{(m,n)}\left(\widetilde{\theta}^\ell, |V|\right)\Big|_{(\widetilde{\theta}^\ell_\star, |V_\star|)}. \end{aligned}$$

Substituting (11) into (16), we get that $\Delta P_{(m,n)} \approx \Psi^\ell_{(m,n)}\Delta\widetilde{P}^\ell$, $\Psi^\ell_{(m,n)} \in \mathbb{R}^{1\times(N-1)}$, where the conventional ISFs in (12) are recovered as the entries of

$$\Psi^\ell_{(m,n)} = -[w_1, w_2] J_\ell^{-1} D_\ell. \tag{17}$$

D. Motivation for Generalized Injection Shift Factors

The derivation of the sensitivity factor in (17) assumes steady-state operation and a predefined slack bus, i.e., bus ℓ. However, a power system exhibits dynamic behaviour, and the notion of a single slack bus that absorbs all power imbalances in the system is only valid for static power-flow analysis. As a result, conventional ISFs do not provide accurate results when system dynamic behaviour is considered, a shortcoming that we exemplify via the following example.

Example 1 (3-Bus System): To illustrate the motivation for deriving generalized ISFs, consider a simple 3-bus system connected in a ring formation. Transmission lines are modelled with lumped parameters, where $y_{12} = 1.3652 - \mathrm{j}11.6041\,\mathrm{p.u.}$, $y^{\mathrm{sh}}_{12} = \mathrm{j}0.088\,\mathrm{p.u.}$, $y_{23} = 0.7598 - \mathrm{j}6.1168\,\mathrm{p.u.}$, $y^{\mathrm{sh}}_{23} = \mathrm{j}0.153\,\mathrm{p.u.}$, $y_{13} = 1.1677 - \mathrm{j}10.7426\,\mathrm{p.u.}$, $y^{\mathrm{sh}}_{13} = \mathrm{j}0.079\,\mathrm{p.u.}$ In this system, generators are connected to buses 1 and 2, injecting $P_1 = 1.5973\,\mathrm{p.u.}$ and $P_2 = 0.7910\,\mathrm{p.u.}$ respectively.

A load is connected to bus 3, with active-power injection $P_3 = -2.35\,\text{p.u.}$ and reactive-power injection $Q_3 = -0.5\,\text{p.u.}$. The voltage magnitude at buses 1 and 2 are regulated at $|V_1| = 1.04\,\text{p.u.}$ and $|V_2| = 1.025\,\text{p.u.}$, respectively.

Suppose bus 1 is set as the slack bus, i.e., $\ell = 1$. Let $\Psi^1_{(m,n)} = [\Psi^1_{(m,n),1}, \Psi^1_{(m,n),2}, \Psi^1_{(m,n),3}]$. Computed using (17), the conventional ISFs for this system are

$$\begin{aligned}\Psi^1_{(1,2)} &= \begin{bmatrix}0 & -0.7529 & -0.2792\end{bmatrix},\\ \Psi^1_{(2,3)} &= \begin{bmatrix}0 & 0.2478 & -0.2792\end{bmatrix},\\ \Psi^1_{(1,3)} &= \begin{bmatrix}0 & -0.2466 & -0.7415\end{bmatrix}.\end{aligned}$$

By definition, the ISFs with respect to the slack bus are 0. On the other hand, if $\ell = 2$, then conventional ISFs are

$$\begin{aligned}\Psi^2_{(1,2)} &= \begin{bmatrix}0.7368 & 0 & 0.2479\end{bmatrix},\\ \Psi^2_{(2,3)} &= \begin{bmatrix}-0.1301 & 0 & -0.4128\end{bmatrix},\\ \Psi^2_{(1,3)} &= \begin{bmatrix}0.4254 & 0 & -0.5037\end{bmatrix}.\end{aligned}$$

The above demonstrates that vastly different numerical ISF values can result depending on the designated slack bus location. The concept of *generalized* ISFs, which do not depend on an arbitrary slack bus, improves upon this. Moreover, Section IV demonstrates that the proposed generalized ISFs can be used to recover conventional ISFs as well as to predict active-power line flows during the transient period between two steady-state operating points. ■

III. Model- and Measurement-based Estimation of Generalized ISFs

Consider the power system model described in Section II-A. Beginning with a valid power flow solution, instead of designating an explicit slack bus ℓ as in the derivation of conventional ISFs (see Section II-C), define the generalized ISF of line (m,n) with respect to bus i as

$$\Gamma_{(m,n),i} := \frac{\partial P_{(m,n)}}{\partial P_i} \approx \frac{\Delta P_{(m,n),i}}{\Delta P_i},\ i \in \mathcal{N}, \tag{18}$$

where ΔP_i denotes small variation in P_i and $\Delta P_{(m,n),i}$ represents the change in active power flow in line (m,n) (measured at bus m) resulting from ΔP_i. Also, collect $\Gamma_{(m,n),i}$'s in the row vector $\Gamma_{(m,n)} \in \mathbb{R}^{1\times N}$. Note that $\Gamma_{(m,n)}$ captures sensitivities with respect to active-power injections at all buses, which is in contrast to $\Psi^\ell_{(m,n)}$ in (17). The remainder of this section details two methods for obtaining the generalized ISFs defined in (18) by: (i) computing them from the AC circuit equations, and (ii) estimating them using active-power injection and flow measurements obtained in real time.

The derivation of the generalized ISF relies on a few preliminaries; these include: (i) a derivation of sensitivities of line-current flows to current injections, (ii) a matrix-based representation of active-power line flows, and (iii) a perturbative analysis of active-power line flows that is agnostic to explicitly designating a slack bus.

A. Current Injection Sensitivities

The derivation of current injection sensitivities begins by rewriting the current through line (m,n) from (13) as

$$I_{(m,n)} = \left(y_{(m,n)} e_{mn}^{\mathrm{T}} + y^{\mathrm{sh}}_{(m,n)} e_m^{\mathrm{T}}\right) V, \tag{19}$$

where $V \in \mathbb{C}^N$ is the vector of bus voltage phasors. If the bus admittance matrix, Y, is invertible,[1] then from (1), the bus voltages can be expressed as $V = Y^{-1} I$. Subsequently, (19) can be written as $I_{(m,n)} = a^{\mathrm{T}}_{(m,n)} I$, where

$$a^{\mathrm{T}}_{(m,n)} = \left(y_{(m,n)} e_{mn}^{\mathrm{T}} + y^{\mathrm{sh}}_{(m,n)} e_m^{\mathrm{T}}\right) Y^{-1} \in \mathbb{C}^{1\times N}. \tag{20}$$

The entries of $a_{(m,n)}$ correspond to the *current injection sensitivity factors* of line (m,n) with respect to the current injection at bus i. Note that the current injection sensitivity factors only depend on network parameters, and not on the operating point.

B. Active-power Injection Sensitivities

Our derivation of the generalized injection shift factors is grounded on computing the sensitivity of a matrix-related expression for the active-power line flows and recognizing their relationship to line currents. To this end, instead of the approach in (14)–(17), we combine (20) together with (14) to obtain

$$S_{(m,n)} = V_m a^{\mathrm{H}}_{(m,n)} I^* = e_m^{\mathrm{T}} V a^{\mathrm{H}}_{(m,n)} I^*. \tag{21}$$

Eliminating I^* from (21) using (3) yields

$$S_{(m,n)} = e_m^{\mathrm{T}} V a^{\mathrm{H}}_{(m,n)} \left(\mathrm{diag}\,(V)\right)^{-1} S. \tag{22}$$

Using the phasor form of the voltages, (22) becomes

$$S_{(m,n)} = \left(|V_m| \angle\theta_m\right) a^{\mathrm{H}}_{(m,n)} \mathrm{diag}\left(\frac{1_{N\times 1}}{|V|\angle\theta}\right) S. \tag{23}$$

Since line power flows are often expressed as functions of angle differences, it is useful to rewrite (23) as

$$\begin{aligned}S_{(m,n)} &= |V_m| a^{\mathrm{H}}_{(m,n)} \mathrm{diag}\left(\frac{1_{N\times 1}\left(1\angle\theta_m\right)}{|V|\angle\theta}\right) S\\ &= |V_m| a^{\mathrm{H}}_{(m,n)} \mathrm{diag}\left(\frac{1_{N\times 1}}{|V|}\angle\left(-\theta^m\right)\right) S,\end{aligned} \tag{24}$$

where $\theta^m = \theta - \theta_m 1_{N\times 1}$. To focus on active-power line flows, it is useful to decompose the current injection sensitivity factors as

$$a_{(m,n)} = \alpha_{(m,n)} + \mathrm{j}\beta_{(m,n)}, \tag{25}$$

which enables us to express the real part of (24) as

$$\begin{aligned}P_{(m,n)} &= e_m^{\mathrm{T}} |V| \left(u^{\mathrm{T}} P + v^{\mathrm{T}} Q\right)\\ &=: p_{(m,n)}(\theta^m, |V|, P, Q),\end{aligned} \tag{26}$$

where

$$u := \mathrm{diag}\left(\frac{\cos\theta^m}{|V|}\right)\alpha_{(m,n)} - \mathrm{diag}\left(\frac{\sin\theta^m}{|V|}\right)\beta_{(m,n)}, \tag{27}$$

[1]The inclusion of the shunt admittance term in (19) intrinsically guarantees invertibility of Y by inducing diagonal dominance [12].

$$v := \operatorname{diag}\left(\frac{\sin\theta^m}{|V|}\right)\alpha_{(m,n)} + \operatorname{diag}\left(\frac{\cos\theta^m}{|V|}\right)\beta_{(m,n)}. \quad (28)$$

Note that $p_{(m,n)}$ in (26) is a function of active- and reactive-power injections at *all* buses. With these preliminaries in place, next we state the main result of this paper.

Consider the active-power flow in line (m,n). Suppose the originating bus m sets the angle reference and the solution to (5) is denoted by $(\theta^m_\star, |V_\star|, P_\star, Q_\star)$. Then, small variations in the active-power flow through line (m,n) are related to small variations in the active-power bus injections by way of $\Delta P_{(m,n)} \approx \Gamma_{(m,n)}\Delta P$, where

$$\Gamma_{(m,n)} = -[r_1, r_2]J_m^{-1}D_m\Pi_m^{\mathrm{T}} + s_1, \quad (29)$$

with $r_1 \in \mathbb{R}^{1\times N-1}$, $r_2 \in \mathbb{R}^{1\times N}$, $s_1 \in \mathbb{R}^{1\times N}$ given by

$$r_1 = e_m^{\mathrm{T}}|V|\left(u^{\mathrm{T}}\Pi_m\operatorname{diag}(\widetilde{Q}^m) - v^{\mathrm{T}}\Pi_m\operatorname{diag}(\widetilde{P}^m)\right), \quad (30)$$

$$r_2 = \left(P^{\mathrm{T}}u + Q^{\mathrm{T}}v\right)e_m^{\mathrm{T}} - e_m^{\mathrm{T}}|V|\left(u^{\mathrm{T}}\operatorname{diag}\left(\frac{P}{|V|}\right) + v^{\mathrm{T}}\operatorname{diag}\left(\frac{Q}{|V|}\right)\right), \quad (31)$$

$$s_1 = e_m^{\mathrm{T}}|V|u^{\mathrm{T}}, \quad (32)$$

and u and v as defined in (27) and (28). The quantities u, v, r_1, r_2, and s_1 are all evaluated at the nominal power flow solution $(\theta^m_\star, |V_\star|, P_\star, Q_\star)$. The derivation of (29) is provided in Appendix A.

The expressions in (29) and (30)-(32) yield sensitivity factors of $P_{(m,n)}$ with respect to entries of the active-power injection vector, P, for a special case. Assume a flat voltage profile, i.e., $|V_i| = 1\,\text{p.u.}$ and $\theta_i \approx 0^\circ$, for all $i \in \mathcal{N}$. With these assumptions, (29) reduces to

$$\Gamma_{(m,n)} = \alpha^{\mathrm{T}}_{(m,n)}. \quad (33)$$

In other words, the power-flow sensitivities reduce to the line current-flow sensitivities, which makes intuitive sense.

C. Measurement-based Estimation of Generalized ISFs

In Section III-B, we derived closed-form expressions for the generalized ISF using an up-to-date model of the system. On the other hand, PMUs, which provide synchronized voltage, current, and frequency measurements as many as 60 times per second [13], enable us to estimate generalized ISFs in real time. For case studies in Section V, a sampling rate of 30 Hz is used. The measurement-based method relies only on inherent fluctuations in measurements of load and generation and is thus adaptive to operating point and topology changes [4]. This section tailors the measurement-based ISF estimation approach proposed in [4] (and further refined in [14]) to obtain generalized ISFs in real-time, using active-power bus injection and line flow measurements.

Let $P_i(t)$ and $P_i(t+\Delta t)$ denote the active-power injection at bus i at times t and $t+\Delta t$, respectively ($\Delta t > 0$ can be interpreted as the PMU sampling period). Define $\Delta P_i(t) = P_i(t+\Delta t) - P_i(t)$ and denote the change in active power flow in line (m,n) resulting from $\Delta P_i(t)$ by $\Delta P_{(m,n),i}(t)$. The generalized ISF, $\Gamma_{(m,n),i}$, can be computed based on the approximation in (18). However, (18) requires $\Delta P_{(m,n),i}(t)$, which is not readily available from PMU measurements. Instead, assume that the net variation in active power through line (m,n), denoted by $\Delta P_{(m,n)}(t)$, is available from PMU measurements. Further, decompose this net variation as the sum of active power variations in line (m,n) due to active-power injection variations at each bus i:

$$\Delta P_{(m,n)}(t) = \sum_{i=1}^{N}\Delta P_{(m,n),i}(t). \quad (34)$$

Substitution of (18) into each term in (34) yields

$$\Delta P_{(m,n)}(t) \approx \sum_{i=1}^{N}\Delta P_i(t)\Gamma_{(m,n),i}. \quad (35)$$

Suppose $M+1$ sets of synchronized active-power bus injection and line flow measurements are available. Let

$$\Delta P_i[k] = P_i((k+1)\Delta t) - P_i(k\Delta t),$$
$$\Delta P_{(m,n)}[k] = P_{(m,n)}((k+1)\Delta t) - P_{(m,n)}(k\Delta t),$$

$k = 1, \ldots, M$; and define

$$\Delta P_{(m,n)} = \begin{bmatrix}\Delta P_{(m,n)}[1] & \cdots & \Delta P_{(m,n)}[M]\end{bmatrix}^{\mathrm{T}},$$
$$\Delta P_i = \begin{bmatrix}\Delta P_i[1] & \cdots & \Delta P_i[M]\end{bmatrix}^{\mathrm{T}}.$$

For ease of notation, let ΔP represent the $M \times N$ matrix $[\Delta P_1, \ldots, \Delta P_i, \ldots, \Delta P_N]$, where N denotes the number of buses in the system; then, it follows that

$$\Delta P_{(m,n)} = \Delta P\Gamma^{\mathrm{T}}_{(m,n)}. \quad (36)$$

If $M \geq N$, then (36) is an overdetermined system. Via weighted least-squares (WLS) estimation, the solution for $\Gamma_{(m,n)}$ can be obtained as [4]:

$$\widehat{\Gamma}^{\mathrm{T}}_{(m,n)} = (\Delta P^{\mathrm{T}}W\Delta P)^{-1}\Delta P^{\mathrm{T}}W\Delta P_{(m,n)}, \quad (37)$$

where $W \in \mathbb{R}^{M\times M}$ is a weighting matrix. Often, W is designed to place more importance on recent measurements and less on earlier ones. Note that, if $W = I_M$, i.e., all measurements within the estimation time window are weighted equally, then (37) reduces to the solution of a least-squares errors (LSE) estimation problem.

The formulation in (37) assumes that all buses are equipped with PMUs. To relax this requirement, consider the intuition that most line flows are significantly affected by only a small set of electrically nearby buses (this intuition is verified in [14]). With this in mind, (37) can be modified so as to reduce the number of required measurement locations in the system. This observation, in combination with the fact that, in a practical large-scale power system, only major transmission corridors are monitored, would greatly reduce the number of PMUs required in the measurement-based ISF estimation method.

IV. Applications of Generalized ISFs

While the derivation of generalized ISFs does not depend on the location of a slack bus or any power allocation schemes, in this section, we show that the generalized ISFs can be used in conjunction with power allocation schemes to

yield meaningful line-flow predictions. Most generally, power allocation schemes are based on the idea of a distributed slack bus, where any system power imbalance is absorbed by several buses [15], [16]. For example, in the context of contingency analysis, multiple generators may respond to a loss in generation or increase in load. Based on this fact, we utilize generalized ISFs to predict the active-power line flows during the transient period following a loss of generation or increase in load. Moreover, conventional ISFs can be recovered as a special case by assuming that a single generator at a designated slack bus absorbs all power imbalances caused by the contingency.

A. Obtaining Participation Factor-based ISFs

Suppose we are interested in the sensitivity of the active-power flow in line (m, n) with respect to a particular injection at bus i, denoted as ΔP_i, and this injection is balanced by some linear combination of injections at other buses, i.e.,

$$\Delta P_j = -\gamma_j \Delta P_i, \ \sum_{j \neq i} \gamma_j = 1. \tag{38}$$

The participation factors γ_j's can be chosen based on insights gleaned from economic dispatch, governor control, or synchronous generator inertia [5]. For example, generator inertia-based participation factors are obtained by defining

$$\gamma_j = \frac{H_j}{\sum_j H_j}, \tag{39}$$

where H_j denotes the inertia of the synchronous generator j in the system [17, Ch. 5]. Similarly, governor participation factors are obtained by defining

$$\gamma_j = \frac{1/R_j}{\sum_j 1/R_j}, \tag{40}$$

where $1/R_j$ represents the steady-state governor gain for generator j [17, Ch. 4]. The participation factors described in (39) and (40) describe realizations of the distributed slack bus based on power-frequency characteristics of generators in the system [5].

Denote by $\Omega_{(m,n),i}$ the sensitivity of $P_{(m,n)}$ with respect to P_i with consideration for generator participation factors. Substitution of (38) into (35) results in $\Delta P_{(m,n)} \approx \Omega_{(m,n),i} \Delta P_i$, where

$$\Omega_{(m,n),i} = \Gamma_{(m,n),i} - \sum_{j \neq i} \Gamma_{(m,n),j} \gamma_j. \tag{41}$$

Similar procedure for measurement-based generalized ISFs yields $\Delta P_{(m,n)} \approx \widehat{\Omega}_{(m,n),i} \Delta P_i$, where

$$\widehat{\Omega}_{(m,n),i} = \widehat{\Gamma}_{(m,n),i} - \sum_{j \neq i} \widehat{\Gamma}_{(m,n),j} \gamma_j. \tag{42}$$

The participation factor-based ISFs in (41) and (42) can be used to predict the transient active-power line flows following a disturbance. Since the inertial response is faster than that of the governor, we expect the inertia-based ISFs obtained using (41) and (42) together with (39) to be valid for a short time after the occurrence of the disturbance. Following this, we expect that the governor-based ISFs obtained using (41) and (42) together with (40) to be valid until participation factors arising from economic dispatch become relevant.

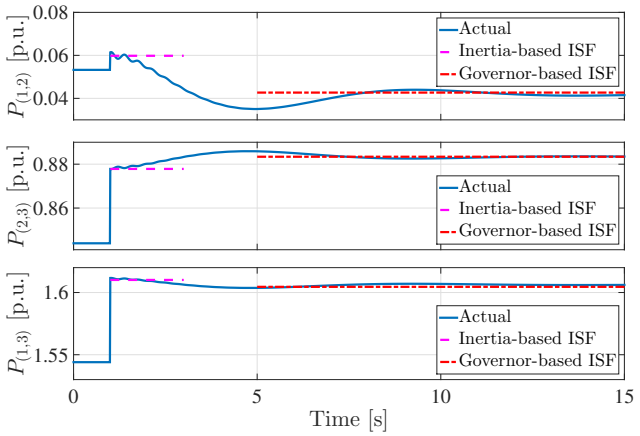

Fig. 1: Line flows in 3-bus system due to a 0.1 p.u. increase in active power demand at bus 3.

B. Obtaining Conventional ISFs

The conventional ISF is simply the sensitivity of the active power flow across line (m, n) with respect to an active-power injection at bus i, which is balanced entirely by the generator at the designated slack bus ℓ, i.e., in the context of (38), $\gamma_\ell = 1$ and all other $\gamma_j = 0$, $j \neq i, \ell$. Thus, as a special case of (41), the conventional ISF can be recovered as

$$\Omega^{\ell}_{(m,n),i} = \Gamma_{(m,n),i} - \Gamma_{(m,n),\ell}, \tag{43}$$

and $\widehat{\Omega}^{\ell}_{(m,n),i}$ can be analogously recovered from (42).

C. Illustrative 3-Bus System Example

In Example 1, we motivated the need to develop generalized ISFs that do not rely on a slack bus. Here, we revisit the 3-bus system from Example 1 and illustrate concepts described in Sections III and IV. First, the current injection sensitivity factors for this system are computed using (20). For each line $(m, n) \in \mathcal{L}$, $a_{(m,n)} = \alpha_{(m,n)} + \mathrm{j}\beta_{(m,n)}$, where

$$\begin{aligned} \alpha_{(1,2)} &= \begin{bmatrix} 0.5178 & -0.2329 & 0.2485 \end{bmatrix}^{\mathrm{T}}, \\ \alpha_{(2,3)} &= \begin{bmatrix} 0.2443 & 0.4934 & 0.0289 \end{bmatrix}^{\mathrm{T}}, \\ \alpha_{(1,3)} &= \begin{bmatrix} 0.4822 & 0.2329 & -0.2485 \end{bmatrix}^{\mathrm{T}}. \end{aligned} \tag{44}$$

For brevity, we refrain from reporting values for $\beta_{(m,n)}$. Next, using (29), generalized ISFs $\Gamma_{(m,n)}$ are computed for each line $(m, n) \in \mathcal{L}$ in this system, to yield

$$\begin{aligned} \Gamma_{(1,2)} &= \begin{bmatrix} 0.5178 & -0.2353 & 0.2493 \end{bmatrix}, \\ \Gamma_{(2,3)} &= \begin{bmatrix} 0.2457 & 0.4934 & 0.0283 \end{bmatrix}, \\ \Gamma_{(1,3)} &= \begin{bmatrix} 0.4822 & 0.2353 & -0.2493 \end{bmatrix}. \end{aligned} \tag{45}$$

Note that, indeed, the generalized ISFs obtained directly above are very similar to $\alpha_{(m,n)}$'s reported in (44). This similarity verifies that, indeed, generalized ISFs can be interpreted as the power analogue of current injection sensitivity factors, as pointed out in (33). Furthermore, like the current injection shift factors, the derivation of generalized ISFs does not depend on a predefined power allocation scheme. To illustrate the flexibility of generalized ISFs, we first verify the validity

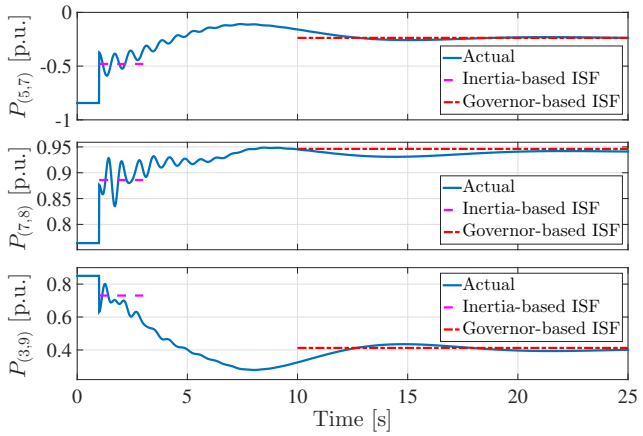

Fig. 2: Line flows in WECC 3-machine 9-bus system due to loss of load at bus 6.

of (43), with bus 1 designated as the slack bus. By using the $\Gamma_{(m,n)}$'s in (45), we obtain

$$\begin{aligned}\Omega^1_{(1,2)} &= \begin{bmatrix}0 & -0.7531 & -0.2685\end{bmatrix},\\ \Omega^1_{(2,3)} &= \begin{bmatrix}0 & 0.2477 & -0.2741\end{bmatrix},\\ \Omega^1_{(1,3)} &= \begin{bmatrix}0 & -0.2469 & -0.7315\end{bmatrix}.\end{aligned} \tag{46}$$

Indeed, the $\Omega^1_{(m,n)}$'s obtained here are very similar to corresponding $\Psi^1_{(m,n)}$'s obtained in Example 1.

Finally, we predict transient active-power line flows using participation factor-based ISFs as given in (41), for a 0.1 p.u. increase in the load at bus 3. To obtain the actual effect due to the 0.1 p.u. active load change disturbance described above, the dynamic simulation tool Power System Toolbox (PST) [18] is used to acquire active-power line flows at pre- and post-disturbance operating points. The load at bus 3 is modelled as a constant-power sink. The synchronous generators at buses 1 and 2 are modelled with the subtransient machine dynamic model equipped with a DC exciter and a turbine governor (see, e.g., [1]). In these models, the rotational inertia are set to $H_1 = 8\,\text{s}$ and $H_2 = 3.01\,\text{s}$ for generators connected to buses 1 and 2, respectively. The governor droop for both generators are set to $1/R_1 = 1/R_2 = 25\,\text{p.u.}$ Based on these parameters, the inertia-based participation factors for the two synchronous generators in the system are $\gamma_1 = 8/11.01$ and $\gamma_2 = 3.01/11.01$. Using these factors in concert with (41), we obtain the change in active power flow through the three lines as $\Delta P_{(1,2)} = 0.0066\,\text{p.u.}$, $\Delta P_{(2,3)} = 0.0339\,\text{p.u.}$, and $\Delta P_{(1,3)} = 0.0661\,\text{p.u.}$ Similarly, the governor-based participation factors are $\gamma_1 = \gamma_2 = 1/2$, and the corresponding changes in power flow are $\Delta P_{(1,2)} = -0.0106\,\text{p.u.}$, $\Delta P_{(2,3)} = 0.0394\,\text{p.u.}$, and $\Delta P_{(1,3)} = 0.0606\,\text{p.u.}$

Simulation results are plotted as the solid trace in Fig. 1. Superimposed onto the actual active-power line flows, we also plot the line flows predicted by the inertia-based and governor-based ISFs in dash and dash-dot traces, respectively. Indeed, we observe that inertia-based ISFs provide a good approximation to the line flows immediately after the load increase, while governor-based ISFs provide a good estimate over longer time horizons.

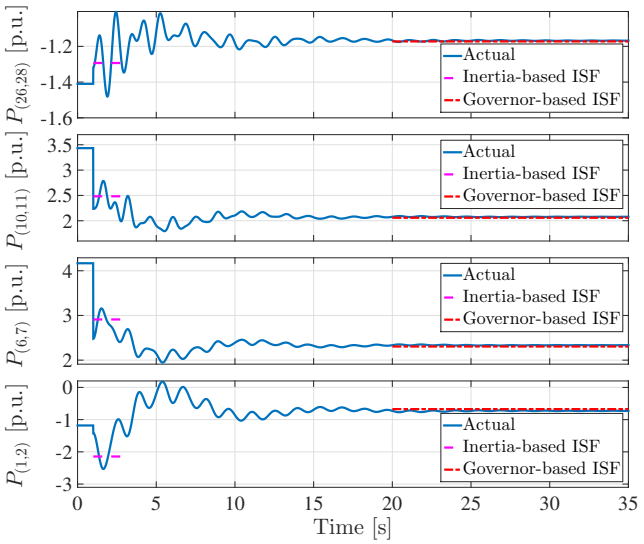

Fig. 3: Line flows in New England system due to loss of load at bus 8.

V. Case Studies

In this section, we illustrate some applications of generalized ISFs with models of the WECC 3-machine 9-bus and the New England 39-bus systems. We compute both conventional and generalized ISFs using the model-based method described in Section III-B. Loads are modelled as constant-power sinks and fluctuations in active-power demand are simulated with the random time-series data:

$$P_i[k] = P_{\text{o},i}[k] + \sigma\nu[k], \tag{47}$$

where $P_{\text{o},i}[k]$ is the nominal active-power load at bus i and $\sigma\nu[k]$ is a pseudorandom number drawn from a normal distribution with 0-mean and standard deviation $\sigma = 0.03\,\text{p.u.}$ We assume a PMU sampling rate of 30 Hz.

A. WECC 3-Machine 9-Bus System Model

Using the pre-contingency base case, we create synthetic power-injection profiles with (47), for $i = 5, 6, 8$, i.e., buses that have loads, which are inherently variable due to the random nature of electricity demand from end users. Using PST, we conduct time-domain dynamic simulations, from which we extract $M = 74$ sets of "measurements" of active-power injections at all buses and flows across all lines. From these simulated measurements, we estimate generalized ISFs using (37) with $W = I_M$, and further compute inertia- and governor-based ISFs via (42). These ISFs are then used to predict active-power line flows in the post-disturbance transient period before a new steady-state is reached.

In this case study, we consider a loss-of-load contingency at bus 6, i.e., $\Delta P_6 = 1.63\,\text{p.u.}$, at time $t = 1\,\text{s}$. We use the same generalized ISFs that were estimated under the pre-contingency pseudo-steady-state operating point. In Fig. 2, line flows predicted by generalized ISFs are superimposed over the dynamic response. Even with the severe loss of load contingency, the generalized ISFs accurately capture post-contingency line flows. As a measure of error, we compute the

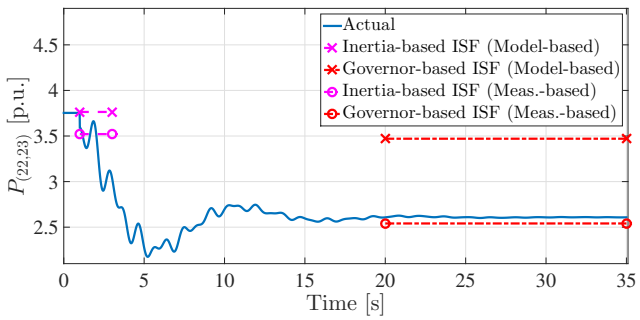

Fig. 4: Line $(22, 23)$ flow in New England system due to loss of load at bus 8, with an undetected outage in line $(16, 21)$. Flows predicted by model-based ISFs are delineated by '$\times$', while those predicted by measurement-based ISFs are delineated by '$\circ$'.

absolute value of the difference between the predicted and actual active-power line flows at $t = 25\,\text{s}$. The average prediction error is $0.004\,\text{p.u.}$, with a maximum error of $0.0061\,\text{p.u.}$

B. New England 39-Bus System Model

This model contains 39 buses and 10 synchronous generators modelled with the subtransient model [1]. All generator models include a governor/turbine and nine include voltage regulators/exciters. To validate the values of generalized ISFs obtained via both the model- and measurement-based methods, we introduce a loss of load contingency at $t = 1$ s, at bus 8, and compare actual post-contingency lines flows with generalized ISF predictions.

1) Base Case: We compute generalized ISFs via (29) using the base-case system circuit model. The average prediction error is $0.0252\,\text{p.u.}$, with a maximum error of $0.0558\,\text{p.u.}$ In Fig 3, we plot actual and predicted post-contingency line flows for a subset of lines.

2) Modified Network: Suppose a line outage has occurred for line $(16, 21)$, unbeknownst to the system operator. In this case, the model-based generalized ISFs from above, which are computed from the base-case network topology, would be inaccurate in predicting line flows for the loss-of-load contingency. The average prediction error is $0.0802\,\text{p.u.}$, with a maximum error of $0.8619\,\text{p.u.}$, corresponding to line $(22, 23)$ flow, as shown in Fig. 4. Such discrepancies can lead to incorrect or suboptimal operating decisions. With this case study, we highlight the advantages of the measurement-based method in Section III-C, which results in generalized ISF estimates that are adaptive to the current system operating point. Indeed, using the measurement-based method, we obtain prediction errors comparable to those reported above in Section V-B1.

VI. Concluding Remarks

In this paper, we introduce the concept of generalized ISF, which can be computed from a sensitivity analysis of the AC circuit equations or estimated using real-time measurements obtained from the system without relying on a model of the system obtained offline. Even though the generalized ISFs are obtained at the pre-disturbance steady-state operating point, we show, through numerical examples and case studies, that they can be easily manipulated to predict active-power line flows during the transient period following a disturbance.

As future work, we will explore dynamic model reduction techniques to obtain time-dependent expressions for participation factors so as to make accurate line flow predictions throughout transients.

Appendix

A. Derivation of the Result in (29)

The result in (29) is derived as follows. Around the nominal power flow solution, $(\theta^m_\star, |V_\star|, P_\star, Q_\star)$, consider small perturbations $\Delta\widetilde{\theta}^m$, $\Delta|V|$, ΔP, and ΔQ. We then get the following expression for small variations in the active-power line flows $\Delta P_{(m,n)}$:

$$\Delta P_{(m,n)} \approx r_1 \Delta\widetilde{\theta}^m + r_2 \Delta|V| + s_1 \Delta P + s_2 \Delta Q, \tag{48}$$

where, with reference to $p_{(m,n)}$ in (26),

$$r_1 = \nabla_{\widetilde{\theta}^m} p_{(m,n)}, \qquad r_2 = \nabla_{|V|} p_{(m,n)},$$
$$s_1 = \nabla_P p_{(m,n)}, \qquad s_2 = \nabla_Q p_{(m,n)}.$$

Substitution of (9) into (48) yields

$$\begin{aligned}\Delta P_{(m,n)} &\approx -[r_1, r_2] J_m^{-1} D_m \Delta\widetilde{P}^m + s_1 \Delta P \\ &\quad - [r_1, r_2] J_m^{-1} E_m \Delta Q + s_2 \Delta Q \\ &= \left(-[r_1, r_2] J_m^{-1} D_m \Pi_m^{\mathrm{T}} + s_1\right) \Delta P \\ &\quad + \left(-[r_1, r_2] J_m^{-1} E_m + s_2\right) \Delta Q \\ &= \Gamma_{(m,n)} \Delta P + \Lambda_{(m,n)} \Delta Q,\end{aligned} \tag{49}$$

where the second equality in (49) follows from the fact that $\theta^m = \theta - \theta_m 1_{N\times 1}$, as defined in (4). Next, expressions for r_1 and r_2 in (30) and (31), respectively, are derived. The derivation begins with the expression for the active-power line flows in (26), which can be rewritten as

$$\begin{aligned}P_{(m,n)} &= |V_m|((\Pi_m^{\mathrm{T}} u)^{\mathrm{T}} (\Pi_m^{\mathrm{T}} P) + (\Pi_m^{\mathrm{T}} v)^{\mathrm{T}} (\Pi_m^{\mathrm{T}} Q)) \\ &\quad + e_m^{\mathrm{T}} \alpha_{(m,n)} P_m + e_m^{\mathrm{T}} \beta_{(m,n)} Q_m \\ &= |V_m| \left(u^{\mathrm{T}} \Pi_m \widetilde{P}^m + v^{\mathrm{T}} \Pi_m \widetilde{Q}^m\right) \\ &\quad + e_m^{\mathrm{T}} \alpha_{(m,n)} P_m + e_m^{\mathrm{T}} \beta_{(m,n)} Q_m \\ &=: \widetilde{p}_{(m,n)}(\widetilde{\theta}^m, |V|, P, Q).\end{aligned} \tag{50}$$

The above expresses the line (m, n) active-power flow in this manner to recover a formulation that is explicitly a function of $\widetilde{\theta}^m$, with respect to which we can differentiate and recover r_1. In particular, with (50) defined above,

$$\begin{aligned}r_1 &= \nabla_{\widetilde{\theta}^m} \widetilde{p}_{(m,n)}(\widetilde{\theta}^m, |V|, P, Q) \\ &= |V_m| \Big(\nabla_{\widetilde{\theta}^m} \left(u^{\mathrm{T}} \Pi_m\right) \mathrm{diag}(\widetilde{P}^m) \\ &\qquad + \nabla_{\widetilde{\theta}^m} \left(v^{\mathrm{T}} \Pi_m\right) \mathrm{diag}(\widetilde{Q}^m) \Big).\end{aligned} \tag{51}$$

Differentiation of u and v in (27) and (28), respectively, with respect to $\widetilde{\theta}^m$ results in

$$\nabla_{\widetilde{\theta}^m} \left(u^{\mathrm{T}} \Pi_m\right) = -v^{\mathrm{T}} \Pi_m, \quad \nabla_{\widetilde{\theta}^m} \left(v^{\mathrm{T}} \Pi_m\right) = u^{\mathrm{T}} \Pi_m. \tag{52}$$

Substitution of (52) into (51) returns r_1 as given by (30). Next, r_2 can be obtained by differentiating the expression in (26) with respect to $|V|$ to yield

$$\begin{aligned} r_2 &= \nabla_{|V|} p_{(m,n)}(\theta^m, |V|, P, Q) \\ &= |V_m| \left(\nabla_{|V|} u^{\mathrm{T}} \mathrm{diag}(P) + \nabla_{|V|} v^{\mathrm{T}} \mathrm{diag}(Q) \right) \\ &\quad + \left[e_m \left(u^{\mathrm{T}} P + v^{\mathrm{T}} Q \right) \right]^{\mathrm{T}}. \end{aligned} \tag{53}$$

From the expressions for u and v in (27) and (28), respectively, we get

$$\begin{aligned} \left(\nabla_{|V|} u^{\mathrm{T}} \right) \mathrm{diag}(P) &= -u^{\mathrm{T}} \mathrm{diag}\left(\frac{P}{|V|} \right), \\ \left(\nabla_{|V|} v^{\mathrm{T}} \right) \mathrm{diag}(Q) &= -v^{\mathrm{T}} \mathrm{diag}\left(\frac{Q}{|V|} \right). \end{aligned} \tag{54}$$

Substitution of (54) into (53) returns r_2 as given by (31). Finally, s_1 and s_2 are obtained directly from differentiating (26) with respect to P and Q as

$$s_1 = \nabla_P p_{(m,n)}(\theta^m, |V|, P, Q) = |V_m| u^{\mathrm{T}}, \tag{55}$$

$$s_2 = \nabla_Q p_{(m,n)}(\theta^m, |V|, P, Q) = -|V_m| v^{\mathrm{T}}. \tag{56}$$

The sensitivities above are all evaluated at the nominal solution of the power flow equations, denoted by $(\theta^m_\star, |V_\star|, P_\star, Q_\star)$. Neglecting ΔQ by setting $\Delta Q = 0_{N\times 1}$ in (49) completes the derivation of (29).

REFERENCES

[1] P. Kundur, *Power System Stability and Control*. New York, NY: McGraw-Hill, Inc., 1994.

[2] U.S.-Canada Power System Outage Task Force. (2004, Apr.) Final report on the august 14th blackout in the united states and canada: causes and recommendations. [Online]. Available: https://reports.energy.gov/BlackoutFinal-Web.pdf

[3] J. Peschon, D. S. Piercy, W. F. Tinney, and O. J. Tveit, "Sensitivity in power systems," *IEEE Transactions on Power Apparatus and Systems*, vol. PAS-87, no. 8, pp. 1687–1696, Aug 1968.

[4] Y. C. Chen, A. D. Domínguez-García, and P. W. Sauer, "Measurement-based estimation of linear sensitivity distribution factors and applications," *IEEE Transactions on Power Systems*, vol. 29, no. 3, pp. 1372–1382, May 2014.

[5] M. Lotfalian, R. Schlueter, D. Idizior, P. Rusche, S. Tedeschi, L. Shu, and A. Yazdankhah, "Inertial, governor, and AGC/economic dispatch load flow simulations of loss of generation contingencies," *IEEE Transactions on Power Apparatus and Systems*, vol. PAS-104, no. 11, pp. 3020–3028, Nov 1985.

[6] A. J. Wood and B. F. Wollenberg, *Power Generation, Operation and Control*. New York: Wiley, 1996.

[7] P. W. Sauer, "On the formulation of power distribution factors for linear load flow methods," *IEEE Transactions on Power App. Syst.*, vol. PAS-100, pp. 764–779, Feb 1981.

[8] FERC and NERC. (2012, Apr.) Arizona-southern california outages on september 8, 2011: Causes and recommendations. [Online]. Available: http://www.ferc.gov/legal/staff-reports/04-27-2012-ferc-nerc-report.pdf

[9] P. W. Sauer, K. E. Reinhard, and T. J. Overbye, "Extended factors for linear contingency analysis," in *Proceedings of the 34th Annual Hawaii International Conference on System Sciences*, Jan 2001, pp. 697–703.

[10] T. Güler, G. Gross, and M. Liu, "Generalized line outage distribution factors," *IEEE Transactions on Power Systems*, vol. 22, no. 2, pp. 879–881, May 2007.

[11] Y. C. Chen, A. D. Domínguez-García, and P. W. Sauer, "Generalized injection shift factors and application to estimation of power flow transients," in *North American Power Symposium (NAPS)*, Sep 2014, pp. 1–5.

[12] R. A. Horn and C. R. Johnson, *Matrix Analysis*. New York, NY: Cambridge University Press, 2013.

[13] US DOE & FERC. (2006, Feb) Steps to establish a real-time transmission monitoring system for transmission owners and operators within the eastern and western interconnections. [Online]. Available: http://energy.gov/sites/prod/files/oeprod/DocumentsandMedia/final_1839.pdf

[14] Y. C. Chen, A. D. Domínguez-García, and P. W. Sauer, "A sparse representation approach to online estimation of power system distribution factors," *IEEE Transactions on Power Systems*, vol. 30, no. 4, pp. 1727–1738, July 2015.

[15] M. Okamura, Y. O-ura, S. Hayashi, K. Uemura, and F. Ishiguro, "A new power flow model and solution method - including load and generator characteristics and effects of system control devices," *IEEE Transactions on Power Apparatus and Systems*, vol. 94, no. 3, pp. 1042–1050, May 1975.

[16] M. S. Ćalović and V. C. Strezoski, "Calculation of steady-state load flows incorporating system control effects and consumer self-regulation characteristics," *International Journal of Electrical Power & Energy Systems*, vol. 3, no. 2, pp. 65–74, 1981.

[17] P. W. Sauer and M. A. Pai, *Power System Dynamics and Stability*. Upper Saddle River, NJ: Prentice-Hall, Inc., 1998.

[18] J. H. Chow and K. W. Cheung, "A toolbox for power system dynamics and control engineering education and research," *IEEE Transactions on Power Systems*, vol. 7, no. 4, pp. 1559–1564, Nov 1992.

Yu Christine Chen (S'10–M'15) received the B.A.Sc. degree in engineering science from the University of Toronto, Toronto, ON, Canada, in 2009, and the M.S. and Ph.D. degrees in electrical engineering from the University of Illinois at Urbana-Champaign, Urbana, IL, USA, in 2011 and 2014, respectively.

She is currently an Assistant Professor with the Department of Electrical and Computer Engineering, The University of British Columbia, Vancouver, BC, Canada, where she is affiliated with the Electric Power and Energy Systems Group. Her research interests include power system analysis, monitoring, and control.

Sairaj V. Dhople (S'09–M'13) received the B.S., M.S., and Ph.D. degrees in electrical engineering, in 2007, 2009, and 2012, respectively, from the University of Illinois, Urbana-Champaign. He is currently an Assistant Professor in the Department of Electrical and Computer Engineering at the University of Minnesota (Minneapolis), where he is affiliated with the Power and Energy Systems research group. His research interests include modeling, analysis, and control of power electronics and power systems with a focus on renewable integration. Dr. Dhople received the National Science Foundation CAREER Award in 2015. He currently serves as an Associate Editor for the IEEE Transactions on Energy Conversion.

Alejandro D. Domínguez-García (S'02–M'07) received the degree of Electrical Engineer from the University of Oviedo, Spain, in 2001, and the Ph.D. degree in electrical engineering and computer science from the Massachusetts Institute of Technology, Cambridge, MA, USA, in 2007.

He is currently an Associate Professor with the Electrical and Computer Engineering Department, University of Illinois at Urbana-Champaign, Urbana, IL, USA, where he is affiliated with the Power and Energy Systems area; he also has been a Grainger Associate since August 2011. He is also an Associate Research Professor with the Coordinated Science Laboratory and in the Information Trust Institute, both at the University of Illinois at Urbana-Champaign. His research interests are in the areas of system reliability theory and control, and their applications to electric power systems, power electronics, and embedded electronic systems for safety-critical/fault-tolerant aircraft, aerospace, and automotive applications.

Dr. Domínguez-García received the National Science Foundation CAREER Award in 2010, and the Young Engineer Award from the IEEE Power and Energy Society in 2012. In 2014, he was invited by the National Academy of Engineering to attend the U.S. Frontiers of Engineering Symposium, and selected by the University of Illinois at Urbana-Champaign Provost to receive a Distinguished Promotion Award. He is an editor of the IEEE TRANSACTIONS ON POWER SYSTEMS and the IEEE POWER ENGINEERING LETTERS.

Peter W. Sauer (S'73–M'77–SM'82–F'93–LF'12) received the B.S. degree from the University of Missouri at Rolla, Rolla, MO, USA, in 1969, and the M.S. and Ph.D. degrees from Purdue University, West Lafayette, IN, USA, in 1974 and 1977, respectively, all in electrical engineering.

From 1969 to 1973, he was an Electrical Engineer on a design assistance team for the Tactical Air Command at Langley Air Force Base, VA, USA, working on design and construction of airfield lighting and electrical distribution systems. He has been on the faculty at the University of Illinois at Urbana-Champaign, Urbana, IL, USA, since 1977, where he teaches courses and directs research on power systems and electric machines. From August 1991 to August 1992, he served as the Program Director for Power Systems in the Electrical and Communication Systems Division, National Science Foundation, Washington, DC, USA. He is a cofounder of the Power Systems Engineering Research Center (PSERC) and has served as the Illinois site director from 1996 to the present. He is a cofounder of PowerWorld Corporation and served as Chairman of the Board of Directors from 1996 to 2001. He is currently the Grainger Chair Professor of Electrical Engineering at Illinois.

Dr. Sauer is a registered Professional Engineer in Virginia and Illinois and a member of the U.S. National Academy of Engineering.